

PAPER • OPEN ACCESS

## Capabilities of the GAMMA-400 gamma-ray telescope for lateral aperture

To cite this article: A V Mikhailova *et al* 2020 *J. Phys.: Conf. Ser.* **1690** 012026

View the [article online](#) for updates and enhancements.



**IOP | ebooks™**

Bringing together innovative digital publishing with leading authors from the global scientific community.

Start exploring the collection—download the first chapter of every title for free.

# Capabilities of the GAMMA-400 gamma-ray telescope for lateral aperture

A V Mikhailova<sup>1</sup>, A V Bakaldin<sup>2</sup>, I V Chernysheva<sup>1,2</sup>, A M Galper<sup>1,2</sup>, M D Kheymits<sup>1</sup>, A A Leonov<sup>1,2</sup>, A.G. Mayorov<sup>1</sup>, V V Mikhailov<sup>1</sup>, P Yu Minaev<sup>2</sup>, S I Suchkov<sup>2</sup>, N P Topchiev<sup>2</sup> and Yu T Yurkin<sup>1</sup>

<sup>1</sup>National Research Nuclear University «MEPhI», Moscow, 115409, Russia

<sup>2</sup>Lebedev Physical Institute, Moscow, 111991, Russia

E-mail: VMikhajlov@mephi.ru

**Abstract.** The future GAMMA-400  $\gamma$ -ray telescope will provide fundamentally new data on discrete sources and spectra of  $\gamma$ -ray emissions and electrons + positrons due to its unique angular and energy resolutions in the wide energy range from 20 MeV up to several TeV. The  $\gamma$ -ray telescope consists of the anticoincidence system (AC), the converter-tracker (C), the time-of-flight system (S1 and S2), the position-sensitive and electromagnetic calorimeters (CC1 and CC2), the scintillation detectors of the calorimeter (S3 and S4) and lateral anticoincidence detectors of the calorimeter (LD). To extend the GAMMA-400 capabilities to measure  $\gamma$ -ray bursts, Monte-Carlo simulations were performed for lateral aperture of the one of the versions of GAMMA-400. Second-level trigger based on signals from CC2, LD, S3, and S4 allows us to detect  $\gamma$ -ray bursts in the energy range of  $\sim 10$ -300 MeV with high effective area about 1 m<sup>2</sup>.

## 1. Introduction

The GAMMA-400  $\gamma$ -ray telescope was developed to solve a broad range of scientific goals, such as precisional searching for high-energy gamma-ray emission when annihilating or decaying dark matter particles and searching for new and studying known Galactic and extragalactic discrete high-energy gamma-ray sources (supernova remnants, pulsars, accreting objects, microquasars, active galactic nuclei, blazars, quasars, etc.) [1, 2]. Another delicate point concerning with the isotropic diffuse  $\gamma$ -ray background (IGRB), which is the most important probes that looks into the energies of the high-energy universe [3, 4]. The dominant sources of the IGRB may be the possible origin of ICECube neutrinos and ultrahigh-energy cosmic rays [5, 6]. Recently, in the sub-TeV energy region MAGIC and HESS experiments observed  $\gamma$ -ray emission denoted as the synchrotron self-Compton (SSC) component in the afterglow phase of  $\gamma$ -ray bursts (GRBs). Thus, significant interest has revealed concerning the observation of GRBs in view of the possible origin of isotropic diffuse  $\gamma$ -ray background in TeV energy region [7]. The GAMMA-400  $\gamma$ -ray telescope is able to investigate time evolution and energy spectra of GRB in the broad energy range from  $\sim 10$  MeV to several GeV.

The GAMMA-400 instrument consists of the anticoincidence system (AC top, AC lat), the converter-tracker (C), the time-of-flight system (S1 and S2), the position-sensitive calorimeter (CC1), electromagnetic calorimeter from columns of CsI(Tl) detectors (CC2), the scintillation detectors of the calorimeter (S3 and S4) and lateral anticoincidence detectors of the calorimeter LD. It is able to



measure high-energy  $\gamma$ -rays on event-by-event basis using main (from the top directions) and additional (from the lateral directions) apertures (figure 1). In this paper the capability of the GAMMA-400 instrument for lateral aperture is presented as the case of  $\gamma$ -ray detection from GRB 190114C, which was investigated in the broad energy range from 1 keV to 1 TeV by the Swift/XRT X-ray telescope, Fermi-LAT  $\gamma$ -ray telescope and MAGIC [8]. Using the GAMMA-400 lateral aperture allows us to observe GRBs in the energy range of  $\sim 10$ -300 MeV from whole sky without the Earth's occultation and away from the radiation belts [9].

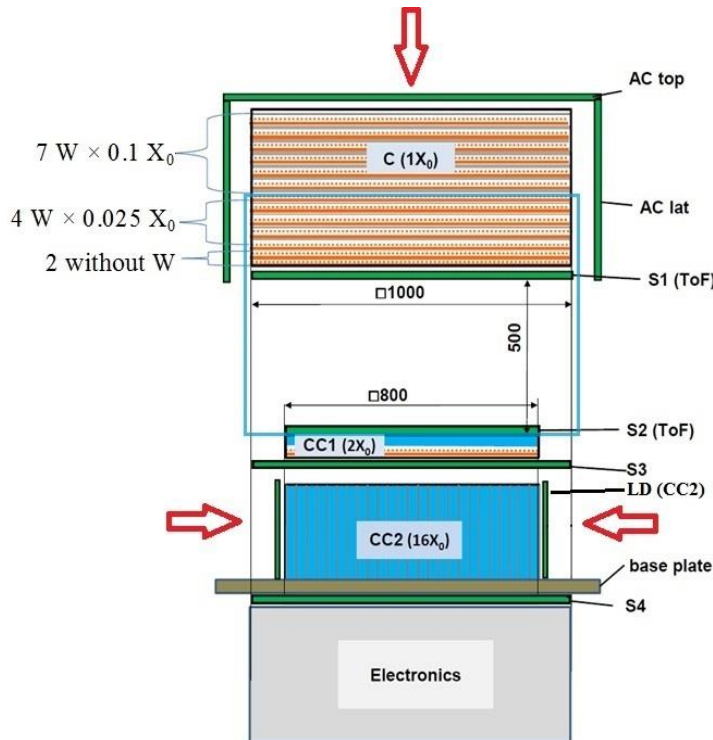


**Figure 1.** One of the versions of physical scheme of the GAMMA-400  $\gamma$ -ray telescope.

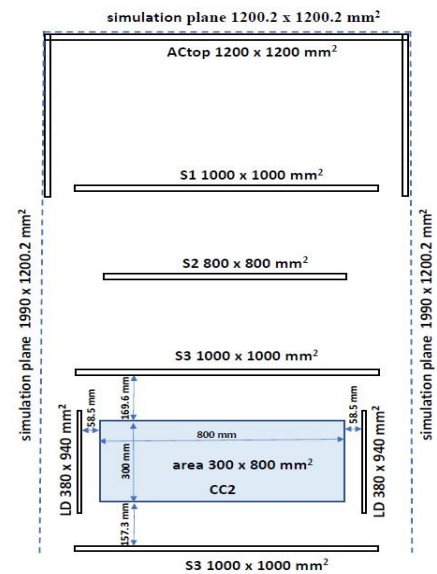


**Figure 2.** Scheme of simulations.

## 2. Simulation

The capabilities of the GAMMA-400  $\gamma$ -ray telescope for lateral aperture were calculated using instrument simulation model [10], processed in GEANT4 environment [11]. The main trigger signal to detect  $\gamma$ -rays captured by lateral aperture is determined as following:

$$\overline{LD} \times \overline{S_3} \times \overline{S_4} \times CC_2 (5 \text{ MeV} < E_{\text{RELEASE}} < 350 \text{ MeV}), \quad (1)$$

where lower limit for the signal in  $CC_2$  is induced by electronic restrictions and upper limit is set due to the data volume concerning the capability of the board data transmitting system. The main point, applying the lateral aperture of the GAMMA-400 instrument to detect  $\gamma$ -rays, is to provide the effective rejection from background cosmic-ray particles, namely: protons, electrons, helium. These charged particles can penetrate inside  $CC_2$  through the holes between lateral detectors LD and scintillation detectors of the calorimeter S3 and S4.

To evaluate the rejection power of selection algorithm the differential isotropic fluxes of cosmic-rays protons [12], electrons [13] and helium [14] obtained from the data of the PAMELA experiment during solar minimum and the differential plane flux of  $\gamma$ -ray from GRB 190114C, averaged over 30 s since beginning of burst [8] were simulated from the different sides of the GAMMA-400 instrument

(figure 2). These fluxes of cosmic rays charged particles and  $\gamma$ -rays from GRB 190114C are presented in figures 3a and 3b, respectively.

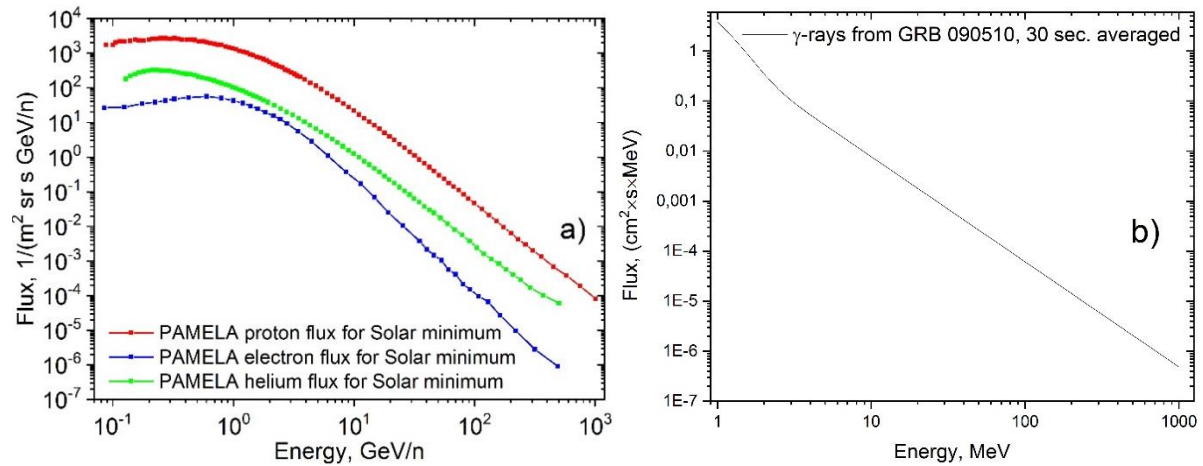


**Figure 3.** The differential isotropic fluxes of cosmic-rays protons, electrons and helium obtained from the PAMELA experiment data during solar minimum (a). The differential plane flux of  $\gamma$ -rays from GRB 190114C averaged over 30 s since beginning of burst (b).

### 3. Results

For selection of  $\gamma$ -rays from charged particles background an additional criteria were applied based on differences in electromagnetic and hadronic cascades in calorimeter CC2. As example, the energy deposit in second row from columns of CsI(Tl) detectors as function of total energy deposit in whole calorimeter CC2 is presented in figure 4 for  $\gamma$ -rays (left) and for protons (right).

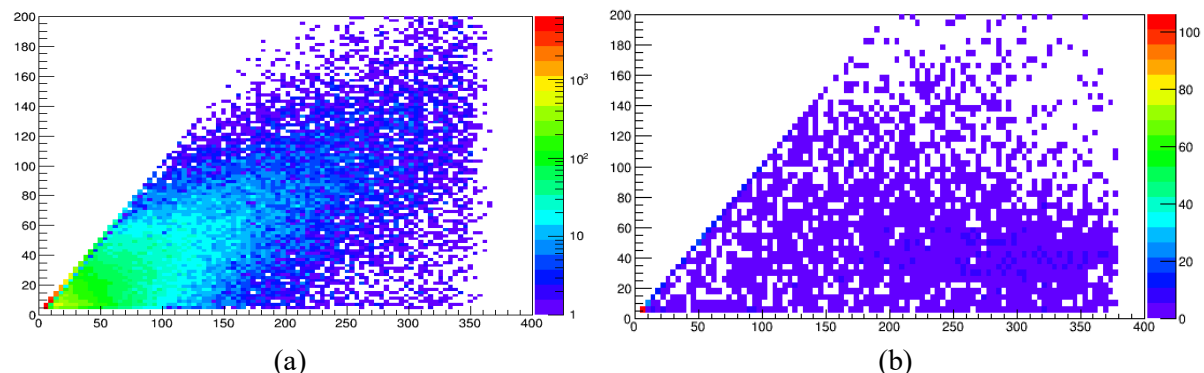


**Figure 4.** The energy deposit in second row from columns of CsI(Tl) detectors as function of total energy deposit in whole calorimeter CC2 for  $\gamma$ -rays (a) and for protons (b).

The acceptance and effective area of  $\gamma$ -ray detection arriving from one lateral side after applying of the main trigger (1) and additional criteria based on differences in electromagnetic and hadronic cascades in calorimeter CC2 are shown in figures 4a and 4b, respectively.

The numbers of detected events from isotropic flux of cosmic rays: electrons, protons and helium nuclei (figure 3a) and from GRB plane flux (figure 3b) during 30 s are estimated and presented in table 1. From this table it is evident, that this GRB is reliably detected from the background in the lateral aperture of GAMMA-400 instrument. The next step will be concerning to the development of the algorithm for  $\gamma$ -ray spectra analysis.

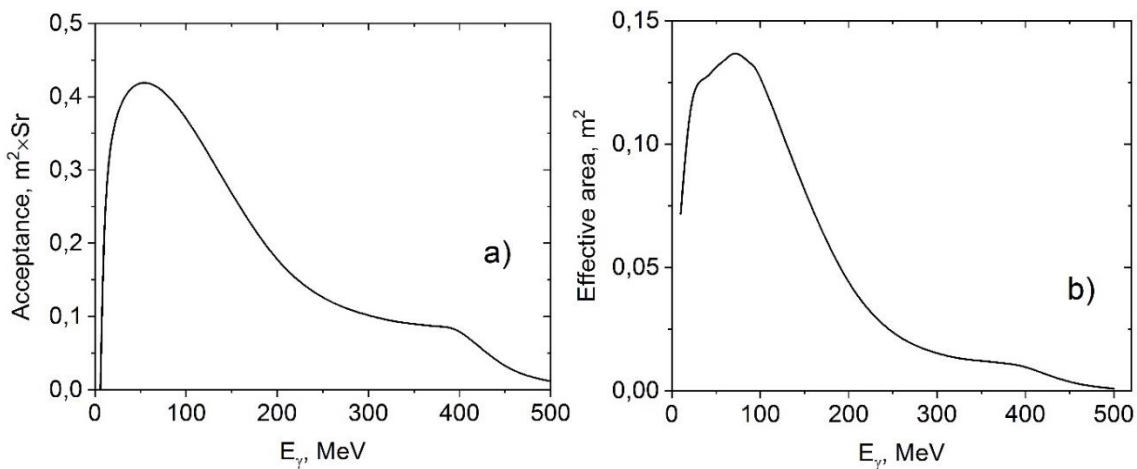


**Figure 5.** The acceptance (a) and effective area (b) of  $\gamma$ -ray detection arriving from one lateral side after applying of the main trigger (1) and additional criteria based on differences in electromagnetic and hadronic cascades in calorimeter CC2.

**Table 1.** The numbers of detected events from isotropic flux of cosmic rays: electrons, protons and helium nuclei (figure 3a) and from GRB 190114C plane flux (figure 3b) during 30 s.

	Events from the main trigger (1)	Events from the main trigger (1) and an additional criteria (% from main trigger)
electrons	2016	171 (8.5%)
protons	81	10 (12%)
helium	176	6 (3%)
gamma (GRB 190114C)	8317	2893 (30%)

### Acknowledgments

This work was partially supported by MEPHI Academic Excellence Project (contract 02.a03.21.0005) and by the Ministry of Science and Higher Education of the Russian Federation under Project "Fundamental problems of cosmic rays and dark matter", No. 0723-2020-0040 and was performed using resources of NRNU MEPHI high-performance computing center.

### References

- [1] Topchiev N P, Galper A M, Bonvicini V *et al.* 2016 *J. Phys.: Conf. Series* **675** 032009
- [2] Topchiev N P, Galper A M, Bonvicini V *et al.* 2016 *J. Phys.: Conf. Series* **675** 032010
- [3] Fornasa M and Sanchez-Conde M A 2015 *Phys. Rep.* **598** 1–58
- [4] Massaro F, Thompson D J and Ferrara E C 2016 *Astron. Astrophys. Rev.* **24** 2
- [5] Waxman E 1995, *Phys. Rev. Lett.* **75** 386
- [6] Hooper D 2016 *JCAP*, **2016** 002
- [7] Yu-Hua Yao, Xiao-Chuan Chang, Hong-Bo Hu *et al.* 2020 *Astrophys. J* **901** 106
- [8] MAGIC collaboration 2019 *Nature* **575** 455-458
- [9] Galper A M, Topchiev N P, Yurkin Yu T, 2018 *Astron. Rep.* **62** 882–889
- [10] Leonov A A *et al.* 2019 *Adv. Space Res.* **63** 3420-3427
- [11] Allison J, Apostolakis J, Lee S B, *et al.* 2016 *Nucl. Instrum. Meth. A* **835** 186-225
- [12] Martucci M *et al.* 2018 *Astrophys. J. Lett.* **854** L2
- [13] Adriani O *et al.* 2015 *Astrophys. J* **810** 142
- [14] Adriani O *et al.* 2011 *Science* **332** 6025